Available online at www.sciencedirect.com
ScienceDirect
Journal of Asian Earth Sciences 29 (2007) 473–489
Journal of Asian Earth Sciences
www.elsevier.com/locate/jaes

Neotectonic fault analysis by 2D finite element modeling for studying the Himalayan fold-and-thrust belt in Nepal

Deepak Chamlagain *, Daigoro Hayashi

Department of Physics and Earth Sciences, University of the Ryukyus, Okinawa 903-0213, Japan

Received 28 December 2004; accepted 25 October 2005

Abstract

This paper examines the neotectonic stress field and faulting in the fold-and-thrust belt of the Nepal Himalaya using the 2D finite element technique, incorporating elastic material behavior under plane strain conditions. Three structural cross-sections (eastern, central and western Nepal), where the Main Himalayan Thrust (MHT) has different geometries, are used for the simulation, because each profile is characterized by different seismicity and neotectonic deformation. A series of numerical models are presented in order to understand the influence of a mid-crustal ramp on the stress field and on neotectonic faulting. Results show that compressive and tensional stress fields are induced to the north and south of the mid-crustal ramp, and consequently normal faults are developed in the thrust sheets moving on the mid-crustal ramp. Since the shear stress accumulation along the northern flat of the MHT is entirely caused by the mid-crustal ramp, this suggests that, as in the past, the MHT will be reactivated in a future large ($M_w > 8$) earthquake. The simulated fault pattern explains the occurrence of several active faults in the Nepal Himalaya. In all models, the distribution of the horizontal σ_1 (maximum principal stress) is consistent with the sequence of thrusting observed in the fold-and-thrust belt of the Himalaya. Failure elements around the flat–ramp–flat coincide with the microseismic events in the area, which are believed to release elastic stress partly during interseismic periods.
© 2007 Published by Elsevier Ltd.

Keywords: Numerical simulation; Main Himalayan Thrust; Stress field; Neotectonics; Nepal Himalaya

1. Introduction

Thin-skinned fold-and-thrust belts are common in orogenic belts of all ages. These zones of folding and thrusting along the margin of a mountain belt constitute one of the most widely recognized and best understood deformational features of the earth. Mechanics of fold-and-thrust belts and accretionary wedges have been extensively studied during the last two decades (Davis et al., 1983; Dahlen, 1990; Lallemand et al., 1994). According to Chapple (1978), the main characteristics of thin-skinned fold-and-thrust belts are: (1) a thin skinned belt, where the limiting horizon is commonly, but not always, close to the crystalline basement; (2) a basal layer of detachment or décollement, composed of weak rock, often shale or evaporite, dipping towards the hinterland; (3) a wedge-shaped region of deformation, thicker in the rear where the thrust originates; (4) large amounts of shortening and thickening in the rear of the wedge.

This thin-skinned belt is usually composed of a series of thrust sheets with the propagation of deformation from the hinterland towards the foreland, and the development of a surface topography sloping towards the foreland. These typical characteristics can be observed in the Himalayan fold-and-thrust belt, which has developed since ca. 50 Ma as a result of the collision between the Indian and Eurasian plates and the subsequent subduction of India beneath the Himalayas. As the Indian Plate has moved continuously towards the north, the sedimentary prism deposited at the northern tip of the Indian Plate has been detached from the underlying basement to form large south vergent thrust sheets, which are bounded by intra-crustal thrusts (Fig. 1).

* Corresponding author. Tel.: +81 906 862 4192; fax: +81 98 895 8552.
E-mail address: dchamlagain@hotmail.com (D. Chamlagain).

1367-9120/$ - see front matter © 2007 Published by Elsevier Ltd.
doi:10.1016/j.jseaes.2005.10.016

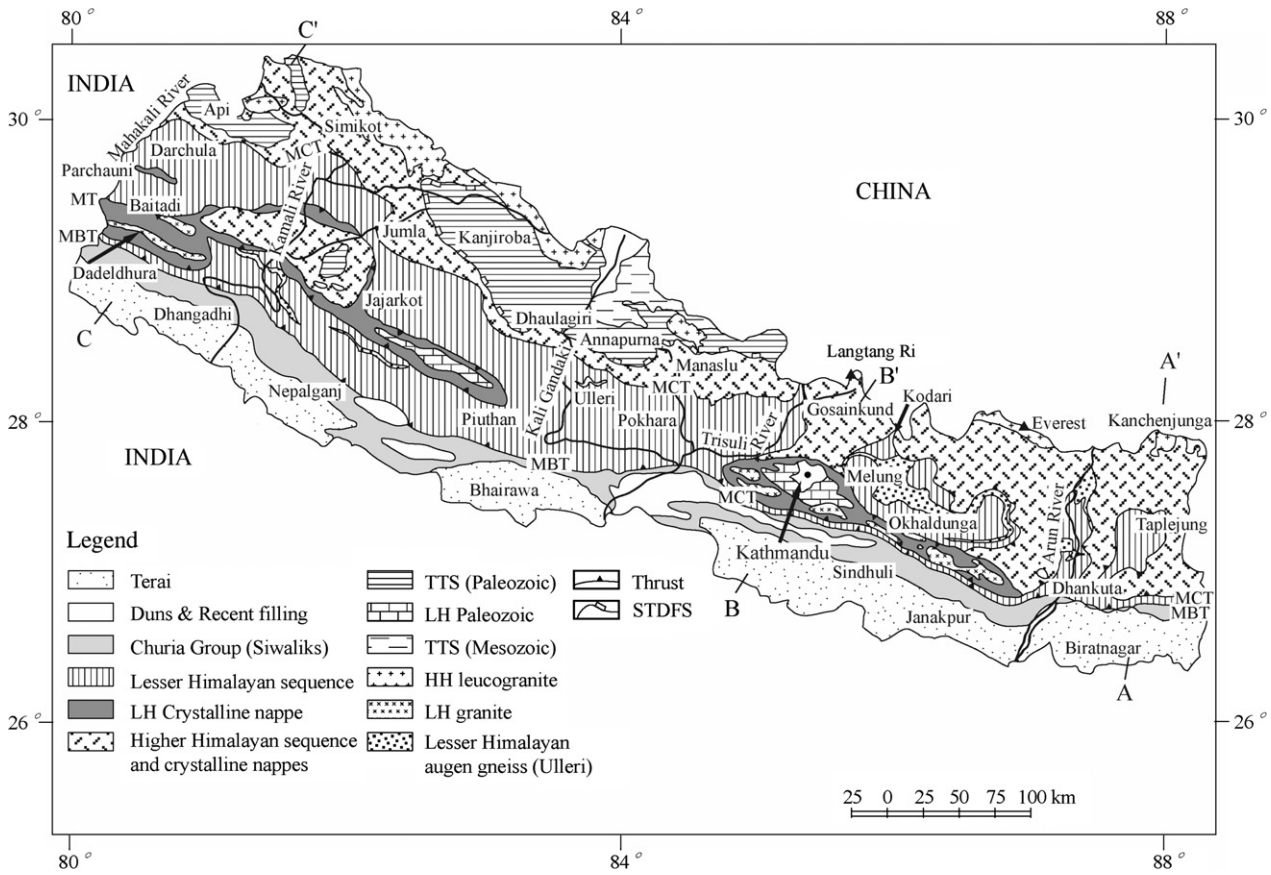


Fig. 1. Geological map of Nepal (modified after Upreti and Le Fort (1999)). LH, Lesser Himalaya; HH, Higher Himalaya; TTS, Tibetan-Tethys sequence; MBT, Main Boundary Thrust; MCT, Main Central Thrust; MFT, Main Frontal Thrust; STDS, South Tibetan Detachment System. A–A′, B–B′, and C–C′: tentative location of the cross-section lines.

From north to south these are the Main Central Thrust (MCT), the Main Boundary Thrust (MBT) and the Main Frontal Thrust (MFT).

Quantitative estimation of the tectonic stress field in the fold-and-thrust belt, both on regional and local scales, is an important constraint for understanding faulting and the resulting geodynamics. In this regard, numerical modeling (Willet et al., 1993; Beaumont et al., 1994; Sassi and Faure, 1997; Mikhailov et al., 2002; Chamlagain and Hayashi, 2004) has been applied extensively to explore the style of deformation and the development of thrust systems during the evolution of the fold-and-thrust belt. Compared to other techniques, numerical techniques allow the modeling of the structure and the deformation at full scale and to compute stress and strain values over a long time period, using various constitutive laws. However, computations are lengthy and require knowledge of the rheological parameters, which are usually poorly constrained. Mäkel and Walters (1993) applied finite element modeling to the study of the mechanics of thrust formation in rectangular and wedge-shaped basins overlying a weak substratum. Using an elastic–plastic law with strain softening characteristics, they obtained a thrust in the rectangular block, and a system of a thrusts and a backthrusts in the tapered wedge, for a relatively small amount of shortening (tens of meters for a 20 km block). Vanbrabant et al. (1999) proposed numerical models for the Variscan fold-and-thrust belt of Belgium to obtain an insight into its evolution. They found that ramps have a significant influence on the development of the belt. For the Himalayan region, Wang and Shi (1982) simulated a 1500 km long section from the Gangetic Plain in the south to Kunlun in the north, using a 2D finite element method under plane strain conditions. Using nonlinear viscous rheology, they predicted a thickening rate ($2\ \mathrm{mm\ yr^{-1}}$) for Tibet, with shortening partitioned across the entire orogen. They proposed that the Himalaya is dynamically supported. Singh et al. (1990) also modeled a cross-section extending from the Ganga Basin to the Tibetan Plateau, aiming to simulate earthquake activity using force rather than displacement boundary conditions. They suggested that the stress concentration indicated by frequent shallow earthquakes in the Himalayan and Tibetan regions is due to force acting from the north side, which is associated with a convection current beneath the Tibetan Plateau. This idea is somewhat controversial in the present state of knowledge of earthquake mechanisms in the Himalaya. Recently, Berger et al. (2004) simulated the interseismic deformations in Nepal Himalaya. They pointed out that the brittle–ductile

transition and geometry of the Main Himalayan Thrust (MHT) are the main factors that influence present-day deformation in the Nepal Himalaya.

Neotectonic studies (Nakata, 1989; Nakata et al., 1990; Mugnier et al., 1994) in the Himalaya have revealed various recent movements (e.g. normal faulting, strike–slip faulting and thrust faulting) along active faults close to the MBT and within the Lesser Himalaya. These movements have been attributed to recent changes in the tectonic regime in the Himalaya. It has also been found that the apparent slip of normal faults close to the intra-crustal thrusts is down to the north, indicating extension. This is not consistent with seismic events of a compressive nature. In this paper, we attempt to clarify the cause of normal faulting in such compressional regimes by applying a 2D plane strain, elastic finite element modeling technique. We further explore the effect of a mid-crustal ramp on the neotectonic stress field in the Nepal Himalaya. Finally, we will compare overall results of the modeling with the record of microseismicity and active faulting in the region to gain a better understanding of the neotectonics of the Nepal Himalaya.

2. Tectonic setting of the Himalayan fold-and-thrust belt

As we mentioned in the previous section, the regional structural geology of the fold-and-thrust belt of Nepal Himalaya to the south of South Tibetan Detachment System (STDS) is controlled mainly by three major thrust systems, e.g. from north to south the MCT, MBT and MFT (Fig. 1). These thrust faults, with a N–S transport direction, are generally inferred to be splay thrusts of the MHT, which marks the underthrusting of the Indian Plate. Most of the cross-sections across the Himalaya suggest a mid-crustal ramp beneath a large antiformal structure of the Lesser Himalaya, and to the north of a synformal structure (Schelling and Arita, 1991; Srivastava and Mitra, 1994; Decelles et al., 2001). Geological, geophysical and structural data indicate that there are lateral variations in the geometry of the MHT (e.g. Zhao et al., 1993; Pandey et al., 1995, 1999), but direct knowledge of the geometry of the MHT is sparse and therefore the validity of the profiles is still in debate.

The MFT system consists of two or three thrust sheets composed entirely of Siwalik rocks; from bottom to top mudstone, multi-storied sandstone and conglomerate. These sedimentary foreland basin deposits provide a record of the final stages of the Himalayan upheaval since ~14 Ma, and also record the most recent tectonic events in the evolution of the Himalaya. In general, this belt exhibits a fault-bend fold structure throughout the Nepal Himalaya. Minor structures include normal faults with centimeter to several meters of displacement. The northernmost thrust sheet of the MFT is truncated by the Lesser Himalayan sequence and overlain by unmetamorphosed to weakly metamorphosed rocks of the Lesser Himalaya, where the Lesser Himalayan rock package is thrust over the Siwalik Group along the MBT. In western Nepal, crystalline thrust sheets are frequently observed within the Lesser Himalaya, e.g. Dadeldhura crystalline thrust sheet (Hayashi et al., 1984). The Lesser Himalayan zone generally forms a duplex above the mid-crustal ramp (Schelling and Arita, 1991; Srivastava and Mitra, 1994; Decelles et al., 2001). The MCT system overlies the Lesser Himalayan MBT system and was formed ca. 24 Ma. This MCT system consists of high-grade rocks, e.g. kyanite–sillimanite gneiss, schist and quartzite, and is characterized mostly by ductile deformation.

3. Active faults in the Nepal Himalaya

The Himalaya is one of the most neotectonically active mountain belts in the world. The active faults, in and around this belt are direct indicators of recent crustal movement due to the collision between the Indian and Eurasian plates. In this section, therefore, active faults and their tectonic significance are reviewed, in order to clarify the neotectonics of the Himalayan fold-and-thrust belt. In the Nepal Himalaya (Fig. 2) active faults, are distributed along the major tectonic elements, as well as along older geological faults, and are classified into four groups (Nakata, 1982): the Main Central Active Fault system, active faults in Lower Himalayas, the Main Boundary Active Fault system and active faults along the Himalayan Frontal Fault (equivalent to MFT). Among these, active faults along the MBT and MFT are most active, and have the potential to produce large earthquakes in the future (Lave and Avouac, 2000; Chamlagain et al., 2000).

The Himalayan front in eastern Nepal is characterized by landforms produced by active faulting, along both the MBT and MFT. Near Timai Khola in eastern Nepal, active faults trending NW–SE along the MBT merge with the active faults striking E–W along the MFT and extending farther south into the Gangetic plain (Fig. 2). These active faults exhibit down-throw towards the north. In central Nepal, traces of active faults are continuous, especially in Hetaunda and south of the Kathmandu valley around the Bagmati River (Chamlagain et al., 2000; Kumahara et al., 2001). Active faults along the MFT also show northward downthrows. Active faulting along the MBT is represented by Arung Khola Fault, the Hetaunda Fault and Udaipur Fault in the east. The traces of these faults are continuous and the north-facing scarplets suggest that they indicate northward dipping fault planes. In western Nepal, active faults along the MBT appear as single, straight, continuous, fault traces at many places. A common topographic feature is a pressure ridge and the vertical slip along the fault is apparently down to the north. Active faults along the MBT, though considered to be basically reverse faults, do not always show a reverse displacement (Nakata et al., 1984), that is active faults close to the MBT are of normal type (Mugnier et al., 1994). Along the MFT, active faults appear to be continuous, as in western Nepal. In the Nepal Himalaya along the Himalayan front, the characteristics of active faults vary from place

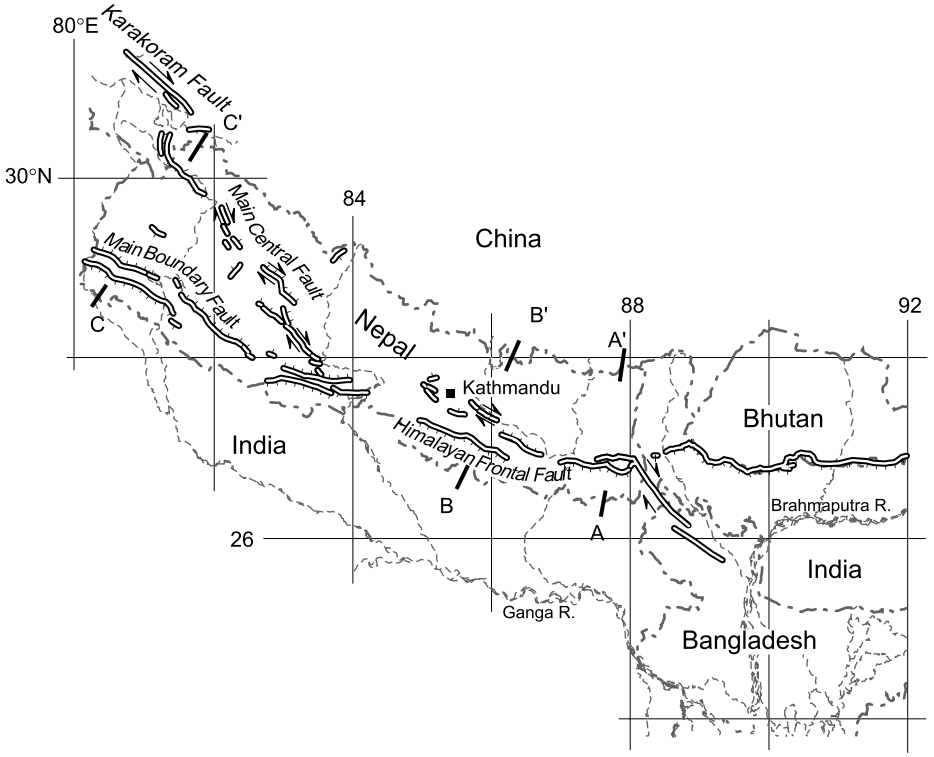


Fig. 2. Active faults in and around Nepal Himalaya. Thick lines without tick marks show newly found active faults. Arrow indicates the direction of strike slip. Down-thrown side is shown by tick marks (after Nakata and Kumahara (2002)). A–A′, B–B′ and C–C′: location of the cross-section lines.

to place, and this is attributed to the difference in the volume of the Siwaliks in different sections of the collision zone. Nakata et al. (1990) obtained the stress field by using the strike and the type of active faults in the collision zone. The stress trajectories show a disturbed pattern near the margin of the Eurasian Plate and are not everywhere consistent with the relative motions of the Indian and Eurasian plates. For the central Himalaya, at least, the stress field shows a horizontal compressive stress consistent with the plate motion. On the other hand, geomorphic analysis shows that the MFT has absorbed, on average, 21 ± 1.5 mm yr^{-1} of N–S shortening south of the Himalaya during Holocene period (Lave and Avouac, 2000). Microseismicity and geodetic data suggest interseismic stress accumulation beneath the Higher Himalayan front, which could in future induce a devastating earthquake ($M_w > 8$). Earthquakes along the MHT can break up to the near surface at the front of the Himalayan foothills and could result in incremental activation of the MFT.

4. Microseismicity

Present-day deformation in the Himalayan fold-and-thrust belt is characterized by large earthquakes (e.g. 1905 Kangra earthquake; 1934 Bihar–Nepal earthquake) of which the magnitude in M_w is ca. 8. These earthquakes appear to be due to ruptures along the MHT. During these events segments of the MHT, 200–300 km along strike and 60–100 km down-dip, are affected by coseismic displacements. The locations of the ruptured areas indicate that there is a gap along the mountain range between the Kangra (1905) and Bihar–Nepal earthquakes (1934) (Fig. 3). In the Himalayan fold-and-thrust belt, focal mechanism data indicates shallow (10–20 km) earthquakes beneath the Lesser Himalaya, demonstrating the activation of thrust planes gently dipping to the north (Ni and Barazangi, 1984). Detailed analysis of the Uttarkashi earthquake (Cotton et al., 1996) in the west of Nepal indicates that this event was initiated to the south of the Higher Himalayan front at 12 ± 3 km depth, corresponding to the southward propagation of a rupture along this segment of the MHT.

Intense microseismicity and moderate earthquake events throughout the Nepal Himalaya cluster along the foothills of the Higher Himalaya (Pandey et al., 1995), forming an E–W trending zone, as shown in Fig. 3. In western Nepal, this cluster lies between 80.5°E and 82.5°E, whereas in central Nepal it lies between longitudes 82.5°E and 86.5°E. The eastern Nepal cluster is characterized by higher level of events between 86.5°E and 88.5°E. The projection of microseismic events into the structural cross-section shows a noticeable change in the shape and location of clusters between central and western Nepal (Fig. 4). In central Nepal, the cluster has a rounded form and is located in the vicinity of the flat-ramp transition of the MHT. The cluster in western Nepal shows an elongate form and is nearly horizontal. These clusters reflect stress accumulation in the interseimic period, during which the décollement beneath the Higher Himlaya probably remained locked with the mid-crustal ramp acting as a geometrical asperity (Pandey et al., 1995).

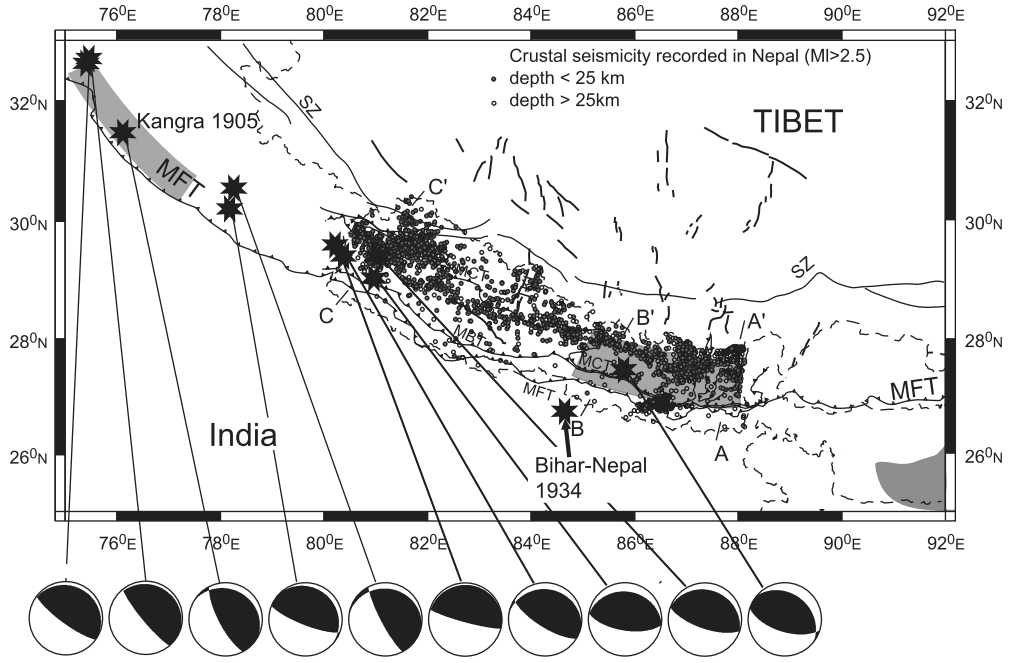


Fig. 3. Seismicity in the Himalayas of Nepal (after Jouanne et al. (2004)). Intense microseismicity (monitored between 1985 and 1998) shown by gray tint and small circles, tend to cluster south of the Higher Himalayas (Pandey et al. (1999)) at mid-crustal level. Stars represent medium size earthquakes. A–A′, B–B′ and C–C′: location of the cross-section lines.

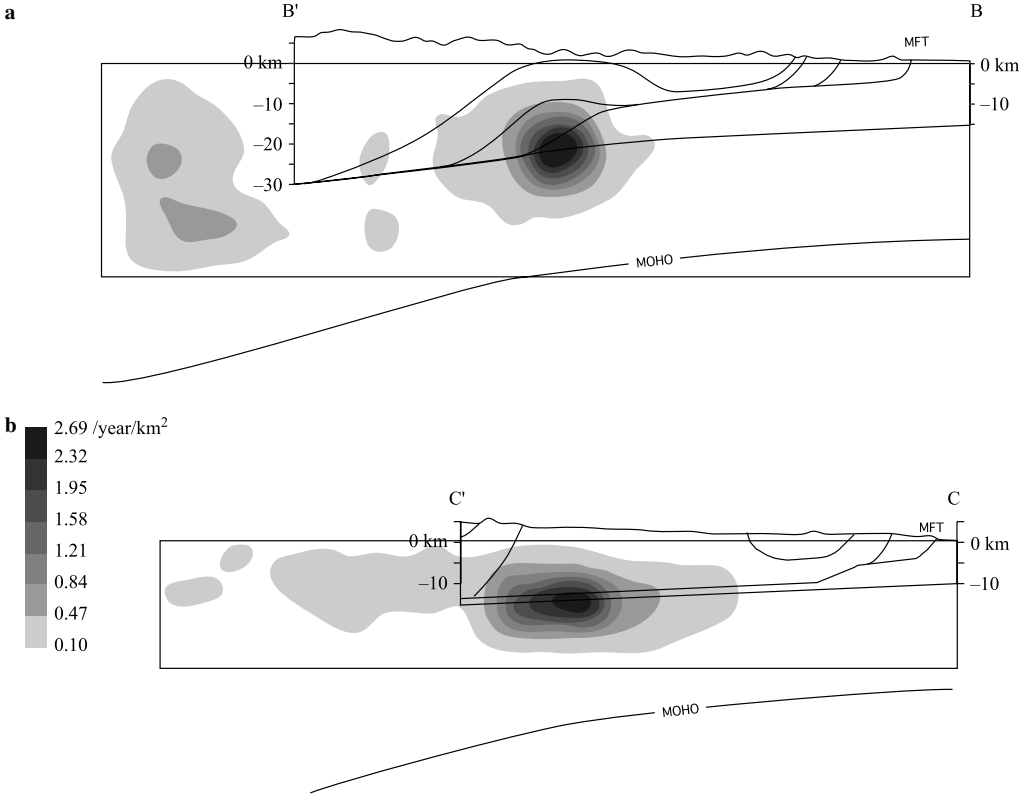


Fig. 4. Density distribution of epicenters (a) central Nepal (b) western Nepal (modified after Pandey et al. (1999)).

5. Simulation of stress and faulting

The neotectonic stress distribution and the resulting faults can be computed using 2D finite element method adopting a simple modeling approach. In this study, we adopt elastic rheology under plane strain conditions. Gravitational force is incorporated in all models. We consider that the MHT is a weak zone, so that it is allocated a

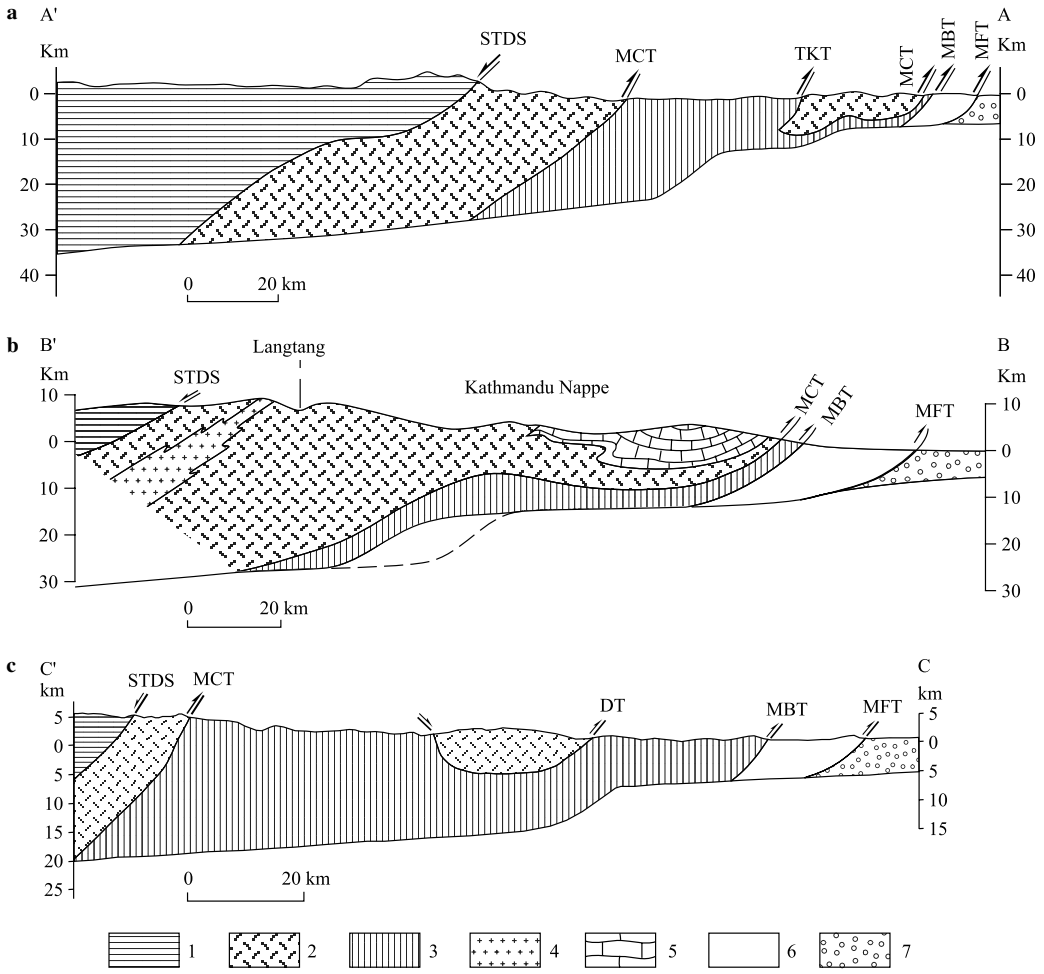


Fig. 5. Geological cross-sections through the Nepal Himalaya at true scale: (a) eastern Nepal (modified after Schelling and Arita (1991) and Zhao et al. (1993)) along A–A′ in Fig. 1; (b) central Nepal (modified after Upreti and Le Fort (1999) and Brunel (1986)) along B–B′ in Fig. 1; (c) western Nepal (modified Decelles et al. (2001)) along C–C′ in Fig. 1. MFT, Main Frontal Thrust; MBT, Main Boundary Thrust; MCT, Main Central Thrust; TKT, Tamar Khola Thrust; DT, Dadeldhura Thrust; STDS, South Tibetan Detachment System. Legend: (1) Tibetan-Tethys sequence; (2) Higher Himalayan Sequence; (3) Lesser Himalayan Sequence; (4) Higher Himalyan leucogranites; (5) Lesser Himalya (Paleozoic); (6) Siwalik; (7) Gangetic plain.

Young's modulus two orders less than that of the other layers, to simulate a weak fault zone subject to slip. This treatment gives a similar effect to the dual-node fault representation technique used by Bott et al. (1989), which was also used successfully by Pauselli and Federico (2003). There is almost no published data on the thickness of the MHT, so we infer from the INDEPTH profile that the MHT zone is about 350 m thick (Zhao et al., 1993).

5.1. Modeling

We consider three typical structural cross-sections through the eastern, central and western Nepal Himalaya (Fig. 5), modified after Schelling and Arita (1991) and Zhao et al. (1993), Upreti and Le Fort (1999) and Brunel (1986) and Decelles et al. (2001), respectively. Each cross-section is divided into six layers (excluding the MHT weak zone), which represent the major structural and lithological units according to their regional tectonic setting (Fig. 6). These units are separated by major faults. All models have different dimensions: for the eastern Nepal model we consider a 212 km long section with a crustal thickness up to 52 km; for central Nepal a 177 km long section up to 50 km thick; and for western Nepal a 148 km long section 37 km thick (Fig. 6). These sections, where the central and western Nepal sections are perpendicular to the clusters of intense microseismicity, include all the tectonic zones of the fold-and-thrust belt. We have prepared one additional model (Fig. 6d) with the same dimensions as the central Nepal model. For this model, we set up a relatively straight MHT, without a mid-crustal ramp, to explore the effect of the ramp on the stress field and the generation of faults. The dip angle of the MHT is 9° towards hinterland. This value is consistent with the INDEPTH results (Zhao et al., 1993).

5.1.1. Eastern Nepal model

The model used for eastern Nepal is based on the structural cross-sections given by Schelling and Arita (1991) and Zhao et al. (1993) and includes a flat–ramp–flat geometry for the MHT. We consider 7, 5 and 30° dips for the

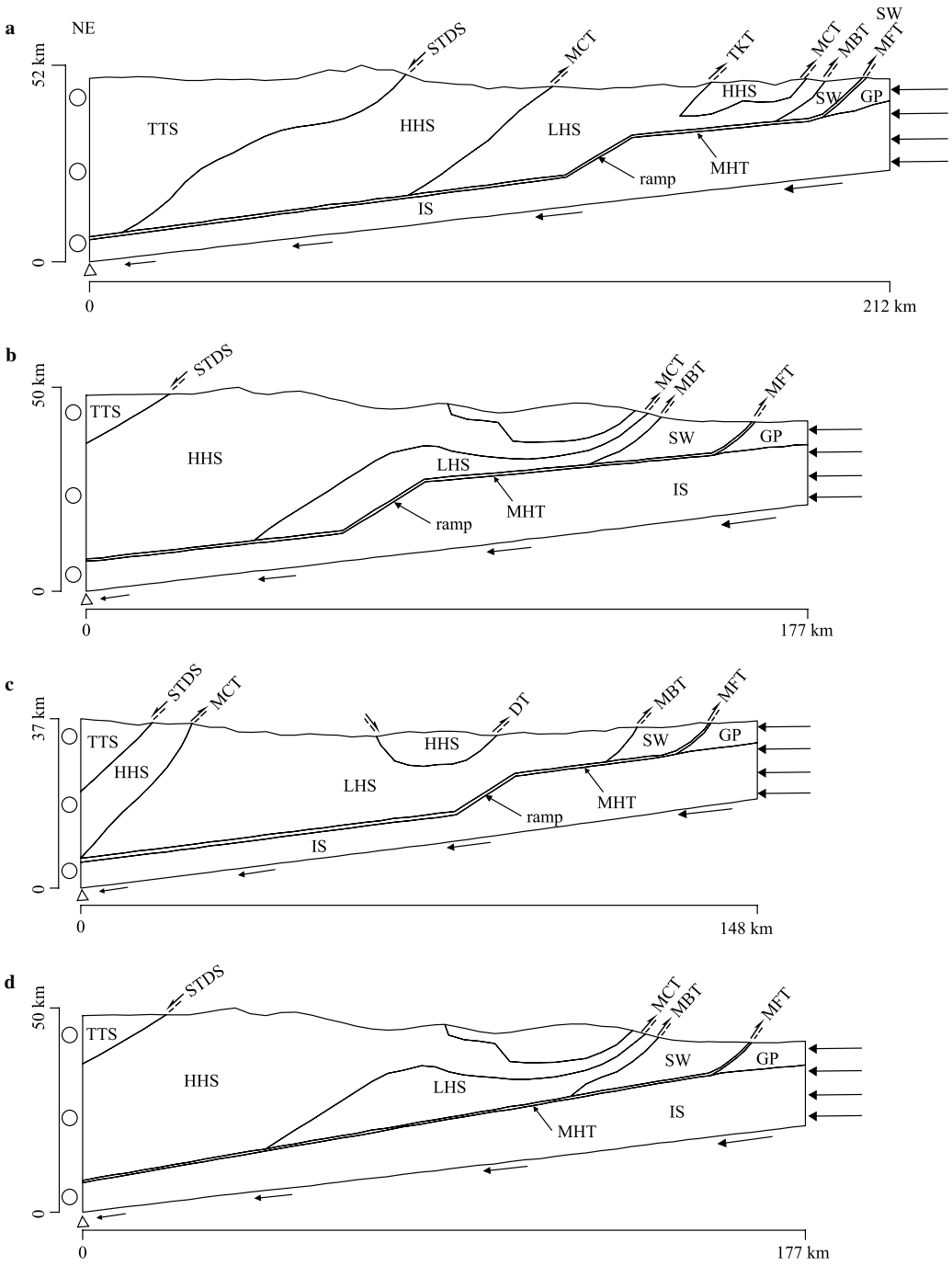


Fig. 6. Geometry and boundary conditions for (a) eastern Nepal model (b) central Nepal model (c) western Nepal model (d) model without ramp. TTS, Tibetan-Tethys sequence; HHS, Higher Himalayan sequence; LHS, Lesser Himalaya–sequence; SW, Siwalik; GP, Gangetic Plain; IS, Indian Shield; STDS, South Tibetan Detachment System; MCT, Main Central Thrust; TKT, Tamar Khola Thrust; DT, Dadeldhura Thrust; MBT, Main Boundary Thrust; MFT, Main Frontal Thrust; MHT, Main Himalayan Thrust.

northern flat, the southern flat and the ramp, respectively, as proposed by Berger et al. (2004) (Fig. 6a). These data are consistent with INDEPTH seismic profile given by Zhao et al. (1993).

5.1.2. Central Nepal model

The central Nepal model is based on the cross-section after Upreti and Le Fort (1999) and the geometry of the MHT is based on Brunel's (1986) cross-section. This geometry has a dip of 5.5° for the northern flat, 5° for the southern flat and 30° for the mid-crustal ramp (Berger et al., 2004) (Fig. 6b).

5.1.3. Western Nepal model

For the western Nepal model, we have taken the structural geometry proposed by Decelles et al. (2001). They

propose only a single mid-crustal ramp along the MHT in western Nepal Himalaya. For computation, we consider the dip of the northern flat, the southern flat and the mid-crustal ramp to be 6, 5 and 30°, respectively (Fig. 6c), based on the dip angles proposed by Berger et al. (2004).

5.2. Boundary conditions

Selection of the boundary conditions is one of the key steps in simulating tectonic processes. In order to match the natural situation, we impose reasonable boundary conditions to represent present-day plate kinematics in the Himalayan fold-and-thrust belt. In all models, the upper surface is free. Since the basal boundary of all models is inclined, the convergent displacement is resolved into both x and y directions, and imposed accordingly. The nodes along the left boundary of each model can only move vertically, whereas from the right side of the models, we impose a convergent displacement at incremental steps, which gradually decrease toward left side of the model. The lowermost node of the left hand side of the model is fixed in each model (Fig. 6). We apply a uniform convergence displacement of up to 500 m, at a rate of 21 mm yr^{-1} for eastern Nepal and 20 mm yr^{-1} for central and western Nepal. These convergence rates are consistent with GPS measurements (Jouanne et al., 2004) and Quaternary displacements (Lave and Avouac, 2000) along the MFT in the Nepal Himalaya.

5.3. Rock layer properties

As mentioned above, for the sake of simplicity in calculation, all models are divided into six layers taking account of the tectonostratigraphy. To calculate the stress field and the resulting deformation in a specific area of the lithosphere, it is essential to know the mechanical properties in that area. In our FEM elastic calculation, we need two independent constants: Young's modulus (E), and the Poisson ratio (v). These parameters are poorly constrained for the Himalayan rocks. Since the density of the major rocks of the each tectonic rock packages is known, we obtain P-wave seismic velocity (V_p) for each rock layer from the diagram proposed by Barton (1986) and compare them with the published velocity model (Pandey et al., 1995) for the Nepal Himalaya. Since we know the density (ρ), V_p and v, the dynamic Young's modulus for each layer can be calculated using equation:

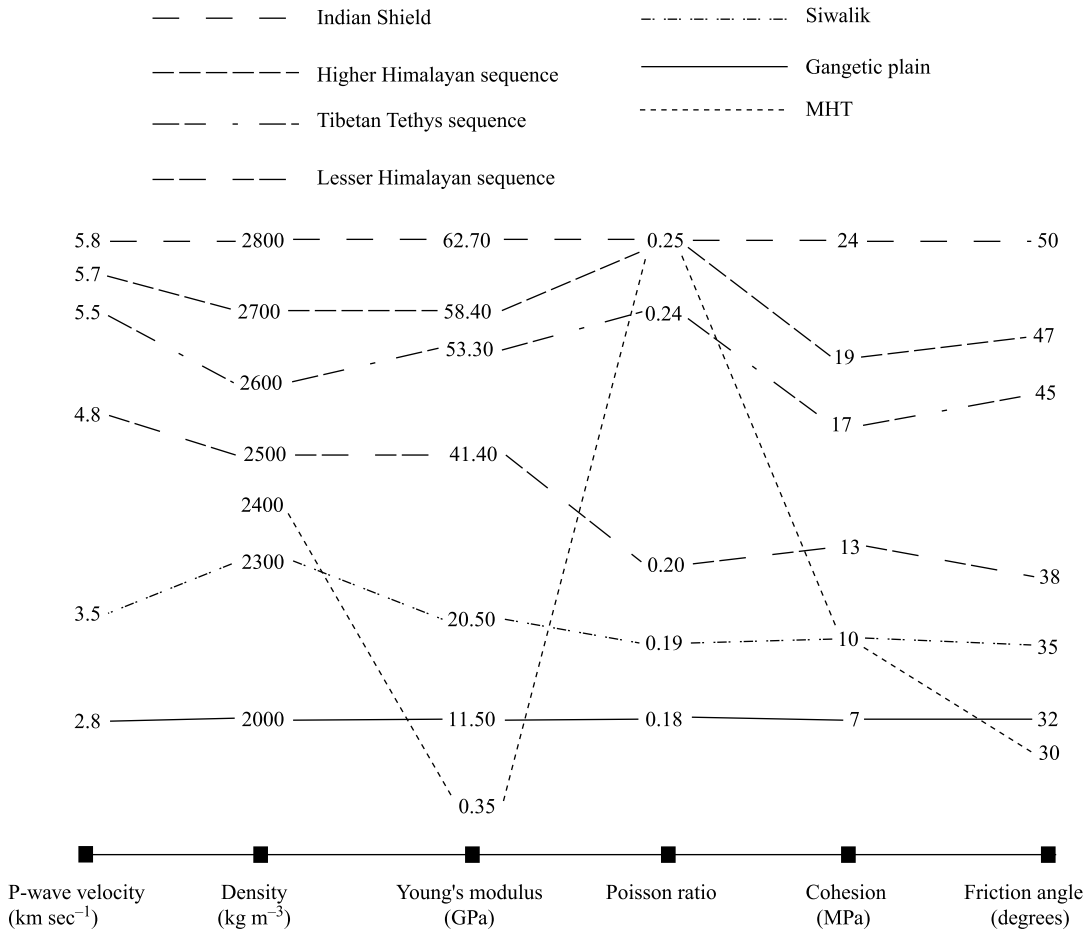


Fig. 7. Rock layer properties.

$$E = \rho V_p^2 \frac{(1+v)(1-2v)}{(1-v)} \quad (1)$$

Assuming that the static Young's modulus is 80% of the dynamic Young's modulus, for calculation we use the static Young's modulus for each tectonic rock unit as shown in Fig. 7. These are consistent with the values for continental crustal rocks determined in the laboratory and with other published data (Sydney and Clark, 1966).

6. Results

Stress state is one of the good proxies for understanding deformation in the crust and depends entirely on the tectonic boundary conditions and the rheology of the rock layers. These constraints also maintain for the Himalayan fold-and-thrust belt, where the state of stress is governed by geometry, tectonic boundary conditions and the convergence rate of the Indian Plate. The MHT is the main structural discontinuity in the Himalaya, its geometry has a significant influence on the changes in the stress field and controls the stress state and the associated deformation. Since the convergence rate of the Indian Plate has been decreasing (Patrait and Achache, 1984) since 40 Ma, the stress field will show consequent changes. Therefore, it is necessary to explore the changes in stress regime with each new tectonic phase, taking into account the changes in the geometry of the structure. In the context of neotectonics in the Himalaya, in the following sections, we will discuss the simulated stress field and the faulting separately, to appreciate differences in each section.

6.1. Results of stress field

We simulate the pattern of the stress field as a function of the model geometry and rock layer properties under various convergent displacements. The simulated stress fields for eastern Nepal, central Nepal and western Nepal are shown in Figs. 8–10, respectively. In general, all models show two characteristic regimes of the stress field under low convergent displacement (50 m): a compressive stress field to the north, and a tensional stress field to the south of the mid-crustal ramp (Figs. 8a, 9a and 10a). The orientation of the stress field is also changed according to the structural characteristics of the model. To the north of the mid-crustal ramp, the stress field shows rotation where σ_1 is deflected from its vertical position and finally becomes horizontal in the upper part of the model. This stress field has the potential to give rise to thrust faulting in a convergent tectonic environment. In contrast, to the south of the mid-crustal ramp, σ_1 is oriented vertically, together with the tensional component of the minimum principal stress (σ_3). In this stress field extensional tectonics will develop. With increasing convergent displacement (500 m) the stress

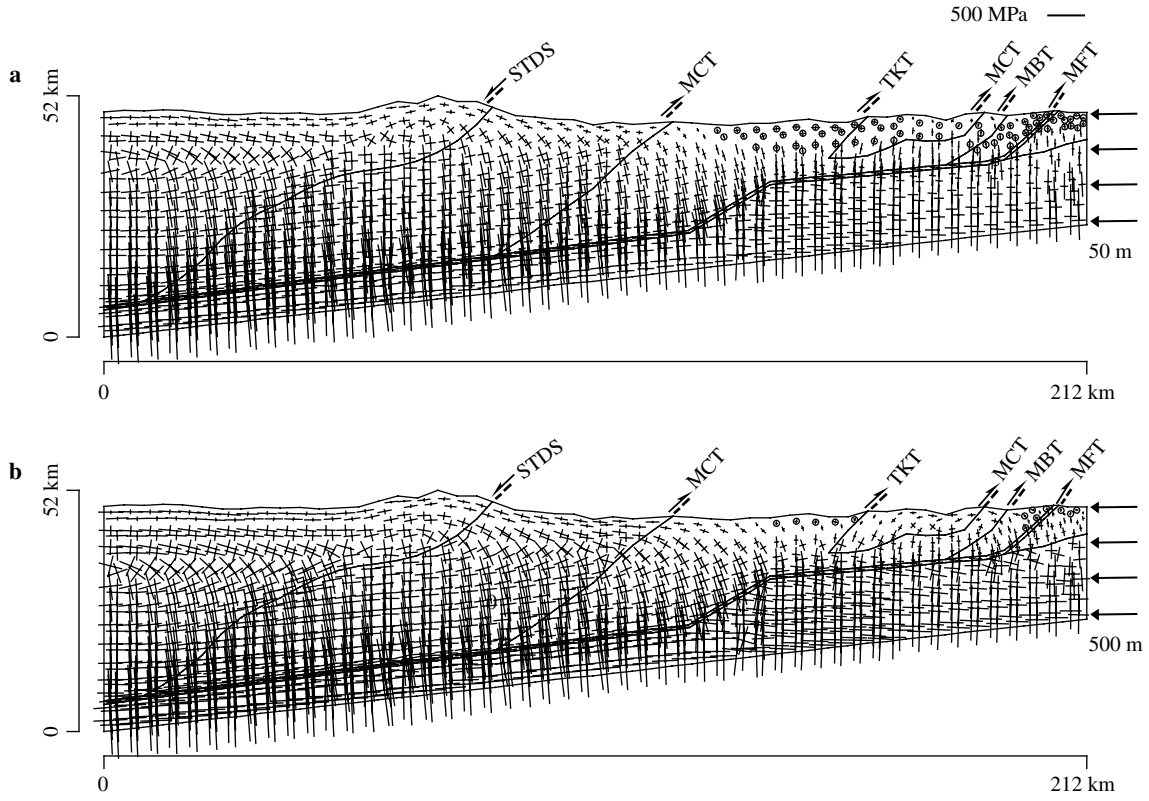


Fig. 8. Stress distribution in the eastern Nepal model: (a) at 50 m convergent displacement; (b) at 500 m convergent displacement. Every pair of perpendicular lines represents σ_1 (long lines) σ_3 (short lines) in the stress field. The tensional stress field is shown by open circles. Abbreviations are same as Fig. 6.

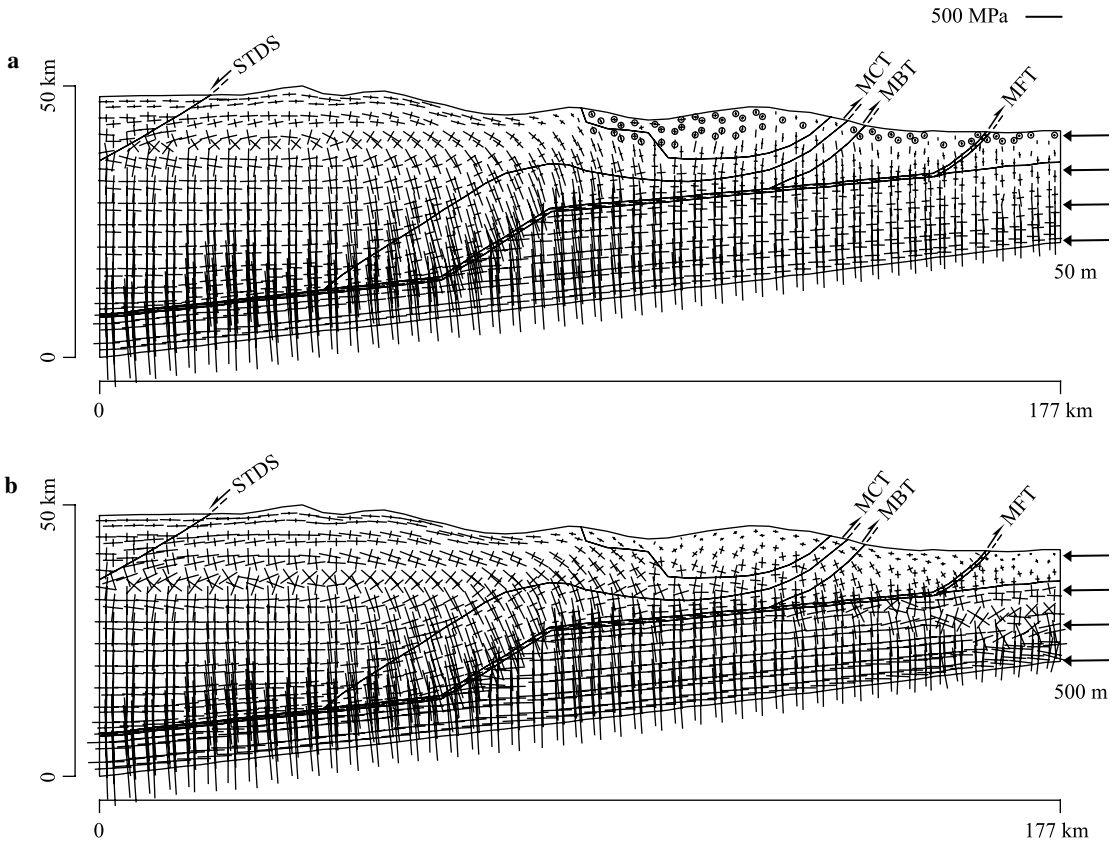


Fig. 9. Stress distribution in the central Nepal model: (a) at 50 m convergent displacement; (b) at 500 m convergent displacement. Every pair of perpendicular lines represents σ_1 (long lines) σ_3 (short lines) in the stress field. The tensional stress field is shown by open circles. Abbreviations are same as Fig. 6.

field changes into a compressive state (Figs. 8b, 9b and 10b) because the stress state is a function of the convergent displacement in such a tectonic setting. Further, the mid-crustal ramp acts as a geometrical asperity, which consequently changes the magnitude of the stress and the orientation of the stress field. The central and western Nepal models, however, still show a tensional stress field to the south of the mid-crustal ramp. In the following sections, we will describe separately the specific features of the stress field in each model.

6.1.1. Eastern Nepal

The tectonic setting and geometry of the eastern Nepal model is different from that of the other models. The Higher Himalayan sequence has been thrust over the Lesser Himalayan sequence along the MCT and a few kilometers to the north a mid-crustal ramp is located beneath this sequence. These differences have induced a distinct stress field. A tensional stress field is prevalent to the south of the mid-crustal ramp (Fig. 8a). Increased convergent displacement has, however, induced a compressive stress field. In the Indian Shield, the orientation of σ_1 remains unchanged as we increase the convergence displacement (Fig. 8b). Shear stress shows a non-uniform distribution (Fig. 11a). The contour of the lowest value (50 MPa) of shear stress extends from north to south at shallow depth. Below this, the shear stress increases gradually, reaching 300 MPa around the northern flat of the MHT.

6.1.2. Central Nepal

The structure and geometry of the central Nepal section, where the Kathmandu Nappe is emplaced above the mid-crustal ramp, is different from the other models. We assume that the rock unit in the core is mechanically equivalent to the Tibetan Tethys sequence and is characterized by a tensional stress field (Fig. 9a). A few elements in the Siwalik also show a tensional stress field. With increasing convergent displacement the stress field changes into compressive state (Fig. 9b). The shear stress shows its lowest value (50 MPa) in two regions: first to the south of the mid-crustal ramp and second at the shallow depth to the north of mid-crustal ramp, where more or less hydrostatic conditions prevail. The northern flat of the MHT shows the maximum (350 MPa) shear stress buildup (Fig. 11b).

6.1.3. Western Nepal

In western Nepal, we consider a single mid-crustal ramp located beneath the Dadeldhura crystalline thrust sheet, which is equivalent to the Higher Himalayan sequence. Comparatively, this model shows more elements with a tensional stress field, mainly distributed in the Lesser Himalayan sequence and in the Siwalik (Fig. 10a). To the

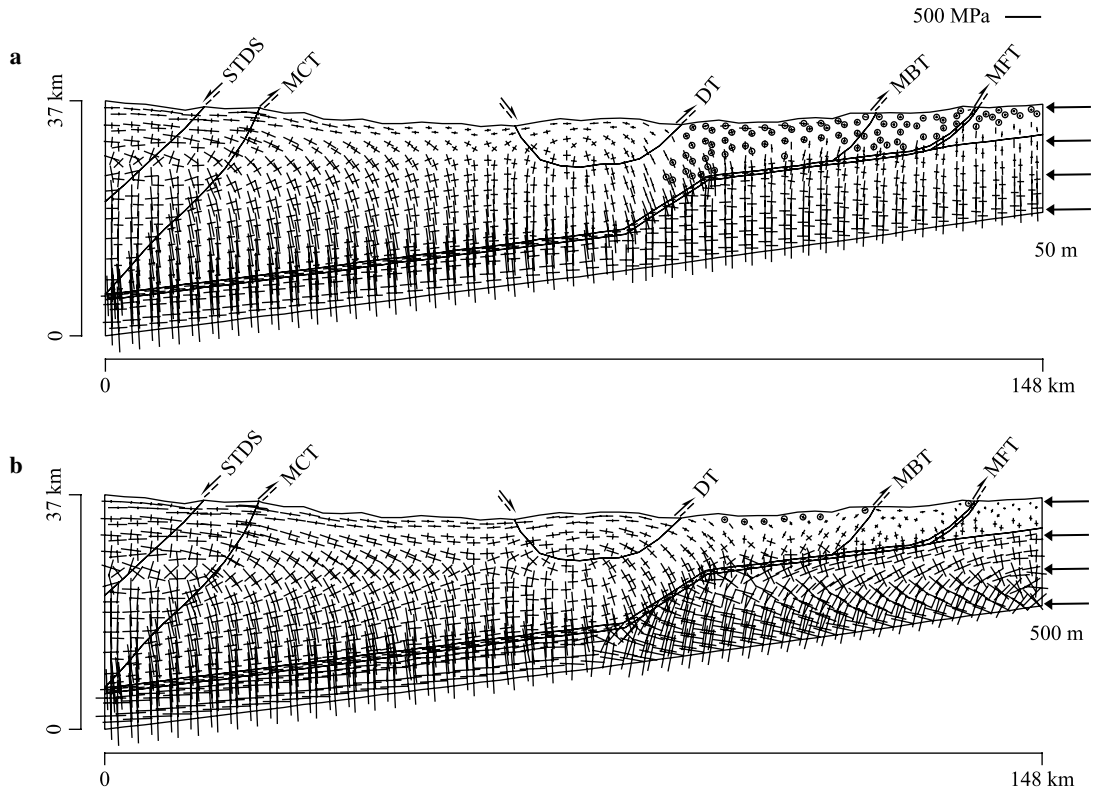


Fig. 10. Stress distribution in the western Nepal model: (a) at 50 m convergent displacement; (b) at 500 m convergent displacement. Every pair of perpendicular lines represents σ_1 (long lines) σ_3 (short lines) in the stress field. The tensional stress field is shown by open circles. Abbreviations are same as Fig. 6.

south of the mid-crustal ramp, the Indian Shield differently shows a compressive state of stress where stress trajectories are rotated, indicating the strong influence of the mid-crustal ramp on the stress state (Fig. 10b). Similarly, to the north of the mid-crustal ramp the σ_1 axis rotates anti-clockwise and finally becomes horizontal. The western Nepal model shows a different shear stress distribution pattern to that of eastern and central Nepal. The contours of the minimum shear stress (50 MPa) are sparsely distributed (Fig. 11c). The magnitude of shear stress reaches up to 250 MPa along the northern flat, less than that in the eastern and central Nepal Himalaya.

6.1.4. Model without mid-crustal ramp

We have also simulated another central Nepal model, without a ramp along the MHT to understand the effect of the ramp on the neotectonic stress field and the development of faults. This model shows very few elements with a tensional stress field (Fig. 12a). Furthermore, the northern flat shows a smaller magnitude of shear stress (300 MPa) than the model with ramp geometry, where in a small area of the model the magnitude of the shear stress reaches 350 MPa (Fig. 11d). Although the difference in shear stress (50 MPa), and its extent is smaller, the overall features of the simulated stress field are different from those of the same model with a ramp geometry, indicating positively the influence of the mid-crustal ramp on the stress field.

6.2. Results of fault distribution

Using well-known Mohr–Coulomb failure criterion, we have computed several failure elements in each section for the eastern, central and western Nepal Himalaya, shown in Figs. 13–15, respectively. In general, all sections show a similar pattern of fault development. Only representative models are described here. Under convergent displacement of 150 m, we observe mostly thrust faults to the north of the mid-crustal ramp, whereas normal faults are extensively developed to the south (Figs. 13a, 14a and 15a). Thrust faults are developed mostly in the Lesser Himalayan and the Higher Himalayan sequences of central and western Nepal Himalaya. Their numbers, however, increase from the eastern to western Nepal Himalaya. Since south of the mid-crustal ramp the stress field is tensional, normal faults are obtained accordingly, distributed mostly in the Lesser Himalayan sequence and in the Siwaliks in eastern and western Nepal. In addition, in central Nepal we also observe normal faults in the core of Kathmandu Nappe (Fig. 14a). Beside these, a cluster of failure elements is observed around the mid-crustal ramp in central Nepal and along the northern flat of the MHT in western Nepal. However, in the eastern Nepal model we could not observe such a cluster of failure elements. With increasing convergent displacement (500 m), the number of failure elements increases to the north of mid-crustal ramp, but decreases to the south (Figs. 13b, 14b and

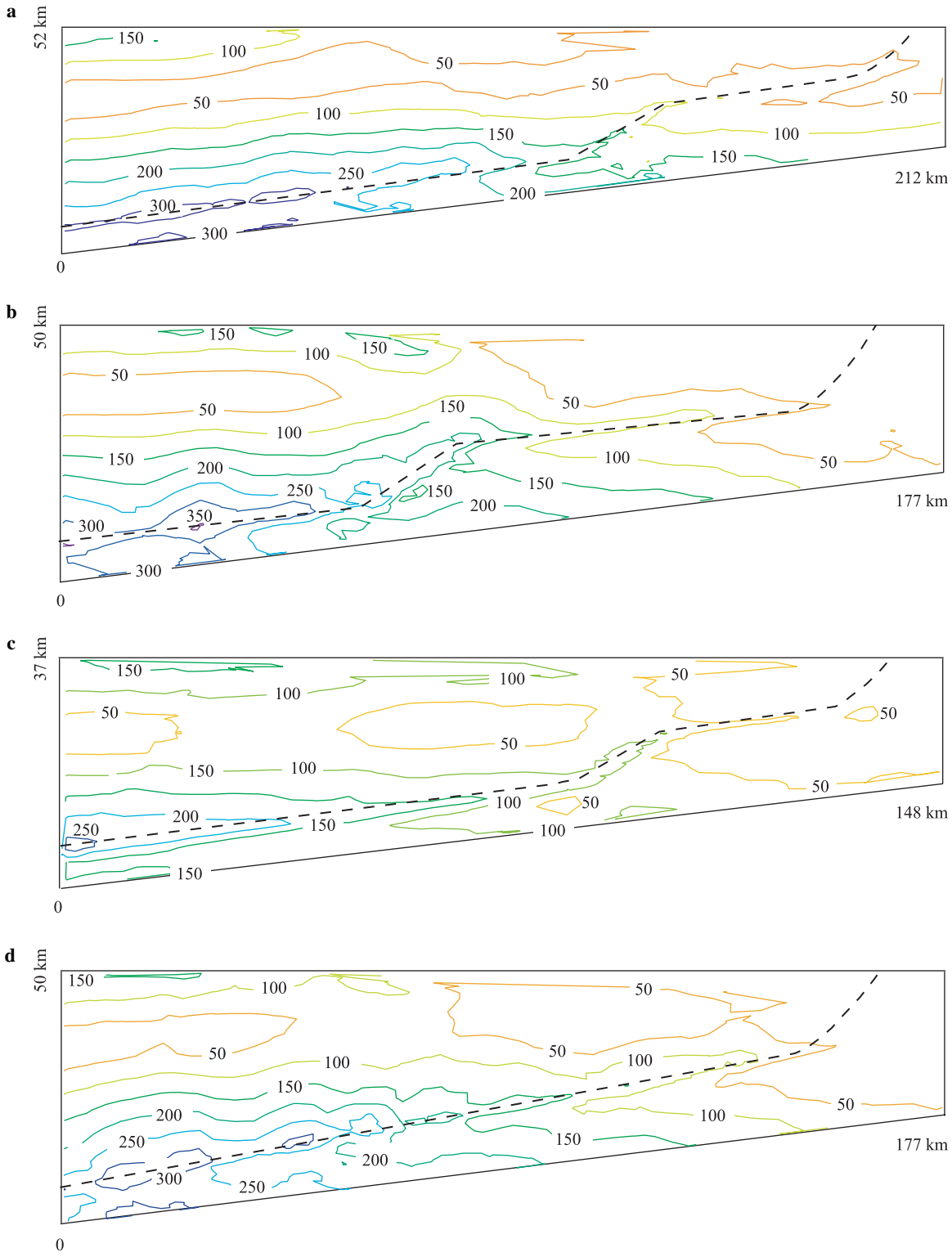


Fig. 11. Shear stress (in MPa) distribution for (a) eastern Nepal (b) central Nepal (c) western Nepal (d) without mid-crustal ramp model at 500 m convergent displacement. Dashed line represents MHT.

15b). Thrust faults are extensively developed in the models for central and western Nepal. The overall pattern demonstrates that thrust faults are propagated from hinterland to foreland as the convergent displacement increases. The model without a mid-crustal ramp predicts relatively fewer failure elements than the model with ramp geometry (Fig. 12b). Similarly, this model is unable to simulate the cluster of failure elements around the mid-crustal level where intense microseismic events are concentrated.

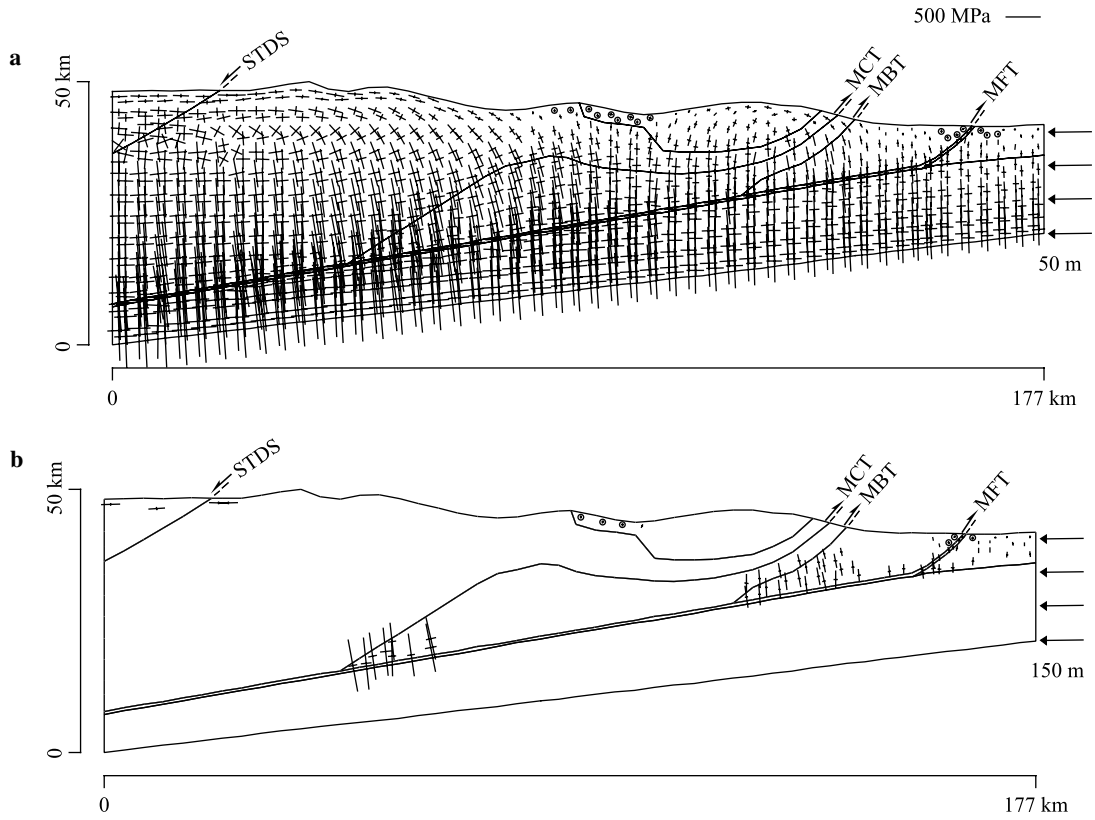


Fig. 12. Model without mid-crustal ramp: (a) stress distribution at 50 m convergent displacement; (b) failure elements at 150 m convergent displacement. Every pair of perpendicular lines represents σ_1 (long lines) σ_3 (short lines) both in the stress field and failure elements. The tensional stress field is shown by open circles. Abbreviations are same as Fig. 6.

7. Discussion

7.1. Modeling assumptions

We have presented a series of 2D finite element models to gain a better understanding of the neotectonics of the fold-and-thrust belt of the Nepal Himalaya using three different structural cross-sections, which are representative of the present-day geometry of the Nepal Himalaya. We have imposed reasonable boundary conditions consistent with the present-day plate kinematics of the region. Further, a convergence displacement has been applied, instead of the forces or stress, because latter are difficult to assess, whereas the relative velocity of the Indian Plate with respect to Eurasian Plate for the Nepal Himalaya is well constrained. All models assume that each layer representing the tectonic rock units is a homogeneous and isotropic body. We have also assumed that the crust behaves elastically by which we can simulate the faulting.

7.2. Neotectonic stress field in Nepal Himalaya

Numerical models, presented herein to explore the neotectonic stress field and faults, have been simplified with respect to structure of the Himalaya and associated plate kinematics. Nevertheless, they still provide a rigorous basis for interpreting the neotectonic stress distribution in relationship to the major structural features, active faults, seismicity and the kinematics of the collison-subduction zone. Nakata et al. (1990) deduced the N–S direction of the maximum horizontal principal stress (σ_{Hmax}) for eastern and central sectors of the Himalaya, using the type and the strike of active faults. They further argued that the direction of σ_{Hmax} is shifted according to a change in the direction of relative plate motion. We have set up the model section plane so that the strike (approximately NE–SW) coincides with σ_{Hmax}.

Our simulated models fall into two categories: a model with ramp geometry along the MHT, and a model without ramp geometry. Models with a mid-crustal ramp show two types of stress field at lower convergent displacement: a compressive stress field north of the mid-crustal ramp, and a tensional stress to the south of the mid-crustal ramp. These states of stress are also maintained with a higher convergent displacement (500 m) in the eastern and western Nepal models. In contrast, a model without a mid-crustal ramp shows a more or less compressive stress field in all regions, which may not be consistent with observations in the tectonically active fold-and-thrust belt, where neotectonics is characterized by active normal faulting in a convergent tectonic setting. Furthermore, the σ_1 axis gradually changes from an inclined to a horizontal position to the north of the mid-crustal ramp. All these results clearly indicate the influence of the mid-crustal ramp on the

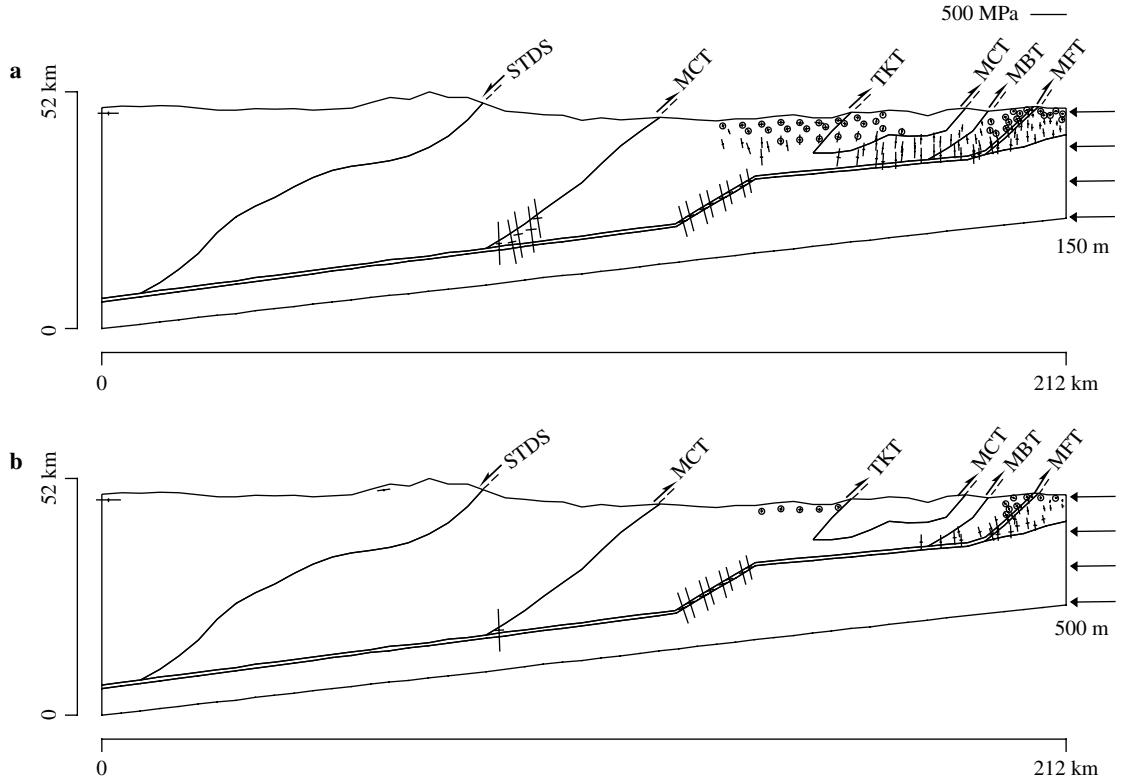


Fig. 13. Failure elements in the eastern Nepal model: (a) at 150 m convergent displacement; (b) at 500 m convergent displacement. Every pair of perpendicular lines represents σ_1 (long lines) σ_3 (short lines) in failure elements. The tensional stress field is shown by open circles. Abbreviations are same as Fig. 6.

stress field. Therefore, both the compressive nature of the stress field with horizontal σ_1 trajectory, and the tensional stress field in thrust sheets displaced above mid-crustal ramp, can be attributed to the effect of the mid-crustal ramp. Taking advantage of the simulated stress field above, we can say that the recent changes in tectonic regime from thrusting to normal and strike slip faulting (Nakata et al., 1990) in the Lesser Himalaya are probably related to the development of the mid-crustal ramp along the MHT. Moreover, the mid-crustal ramp is believed to act as a geometrical barrier to a change in the orientation of σ_1 in the Himalaya. The computed stress field to the north is compatible with the stress field predicted by earthquake focal mechanism solutions in the Himalaya. Similarly, the model with a ramp geometry clearly shows a maximum accumulation of shear stress along the northern flat of the MHT, suggesting an active role for the mid-crustal ramp during interseismic periods. This is consistent with other studies: e.g. numerical simulation (Cattin and Avouac, 2000; Vergne et al., 2001; Berger et al., 2004), seismicity (Pandey et al., 1995) and GPS measurements (Jouanne et al., 2004). The concentration of shear stress along the northern flat of the MHT means that it is likely to be reactivated in a future devastating earthquake ($M_w > 8$), as in the past (compare Figs. 11, 12, 14 and 15 with Fig. 4). This study, therefore, clearly shows the style of stress buildup in the Himalaya during interseismic periods and the significance of this stress pattern for the neotectonic deformation of the region.

7.3. Neotectonic faults in Nepal Himalaya

To gain better understanding of neotectonic movements in the existing stress field, we have carried out fault analysis using the Mohr–Coulomb failure criterion. We have computed failure elements for the three cross-sections of the Nepal Himalaya using the simulated stress field and taking into account the possible mechanical properties, i.e. friction angle and cohesion. We have also simulated another model without ramp geometry, which did not produce a realistic fault pattern. Our models have predicted two types of fault: thrust faults to the north of the mid-crustal ramp and normal faults to the south. In all models, thrusts are propagated towards the foreland as we increase the convergent displacement. This is a characteristic feature of thrust propagation in fold-and-thrust belts. It is also observed that once an element failed in the thrust mode, σ_1 trajectories in the failure element rotate to a more or less horizontal position, which has some bearing on the formation of imbricate thrusts. For such situation, Mandl and Shippam (1981) have argued that the rotation of the stress trajectories would allow the transfer of the push, and facilitate the formation of imbricate thrusts further ahead of the moving thrust sheet. Therefore, in this connection, the rotation of the σ_1 trajectory in failure elements in all models may have had a significant influence in the development of an imbricate thrust system in the Himalayan fold-and-thrust belt.

Clusters of failure elements have been computed around the flat–ramp–flat region of the MHT, which coincide with

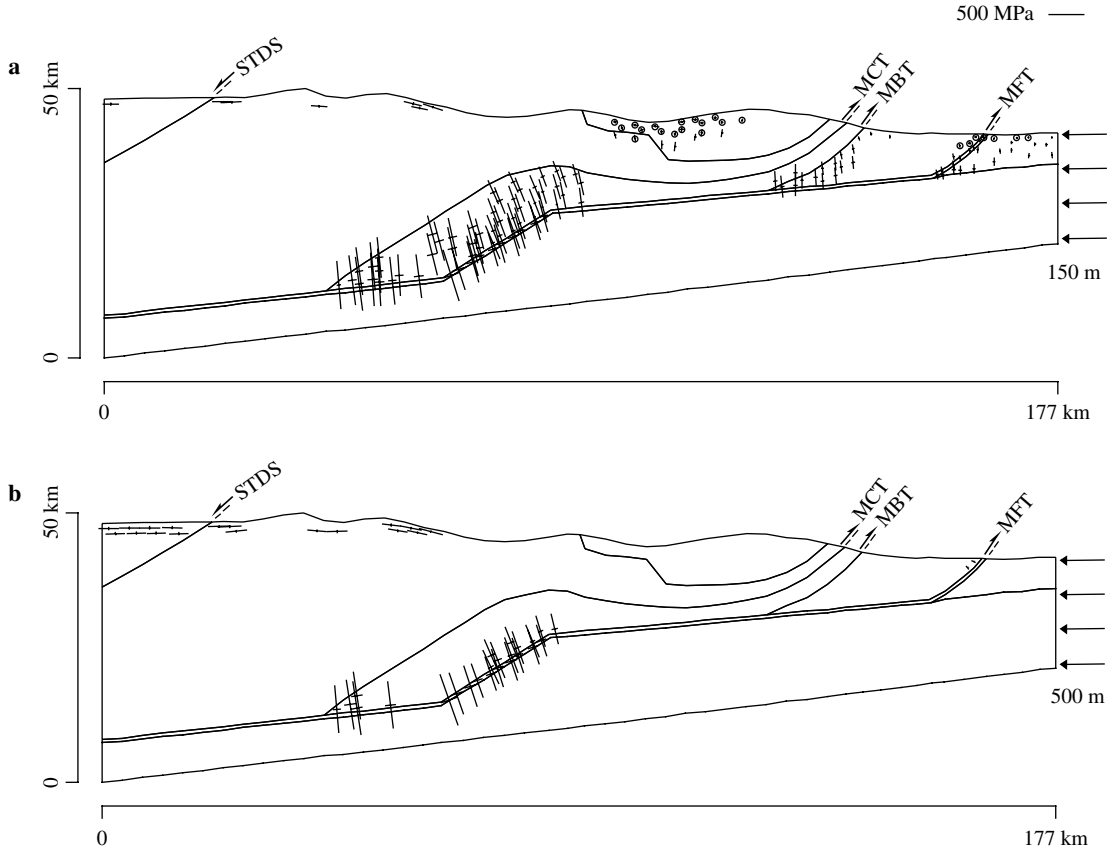


Fig. 14. Failure elements in the central Nepal model: (a) at 150 m convergent displacement; (b) at 500 m convergent displacement. Every pair of perpendicular lines represents σ_1 (long lines) σ_3 (short lines) in failure elements. The tensional stress field is shown by open circles. Abbreviations are same as Fig. 6.

the clusters of microseismic events observed along the Higher Himalayan front, except in the eastern Nepal model, where the cluster of failure elements is quite far from the cluster of the microseismic events, so that there are very few failure elements along the northern flat. In contrast, numerous failure elements have been observed in central Nepal around the mid-crustal ramp, and along the northern flat in the western Nepal model, corresponding with the microseismicity of the region. It is believed that microseismic events around the mid-crustal ramp partly release the interseismic stress accumulated around the ramp. However, the ramp and flat are only activated during a huge earthquake and allowing the transfer of nearly all the interseismic deformation to the most frontal structures (Pandey et al., 1995; Lave and Avouac, 2000). In this regard, our results have some implications for interseismic deformation. Above the mid-crustal ramp and in the southern part of all the models, active deformation is characterized by normal faulting. Furthermore, numbers of active normal faults with a strike slip component have also been reported (Nakata, 1989; Nakata et al., 1990; Mugnier et al., 1994; Saijo et al., 1995), at least in the Nepal Himalaya. This observation is in good agreement with the simulated stress field and fault pattern. Similar fault patterns have also been predicted within a thrust sheet deformed above a ramp, using analytical calculation (Wiltschko, 1979) and numerical modeling (Erickson et al., 2001). The nature of the stress field and the resulting fault pattern to the south of the mid-crustal ramp are in good agreement with the neotectonic model of Nakata et al. (1990), in which they predict that the Lesser Himalayan block is subsiding due to a change in the tectonic regime. Thus our models are able to show the effect of mid-crustal ramp on the neotectonic stress field and the distribution of faulting in the fold-and-thrust belt of the Nepal Himalaya. However, we cannot rule out the influence of the strength contrast between the décollement and the displaced thrust sheet, pore water pressure and décollement slope, which can lead to a new type of inversion, in which the tectonic regime changes from thrust faulting into normal thrusting.

8. Conclusions

The neotectonic stress field and resulting faults have been numerically modeled using 2D finite element method. Our models are based on present-day cross-sections of eastern, central and western Nepal Himalaya with different geometries of the MHT as revealed by structural and geophysical data. The results presented in this study are first-order estimates. The results are compared with records of

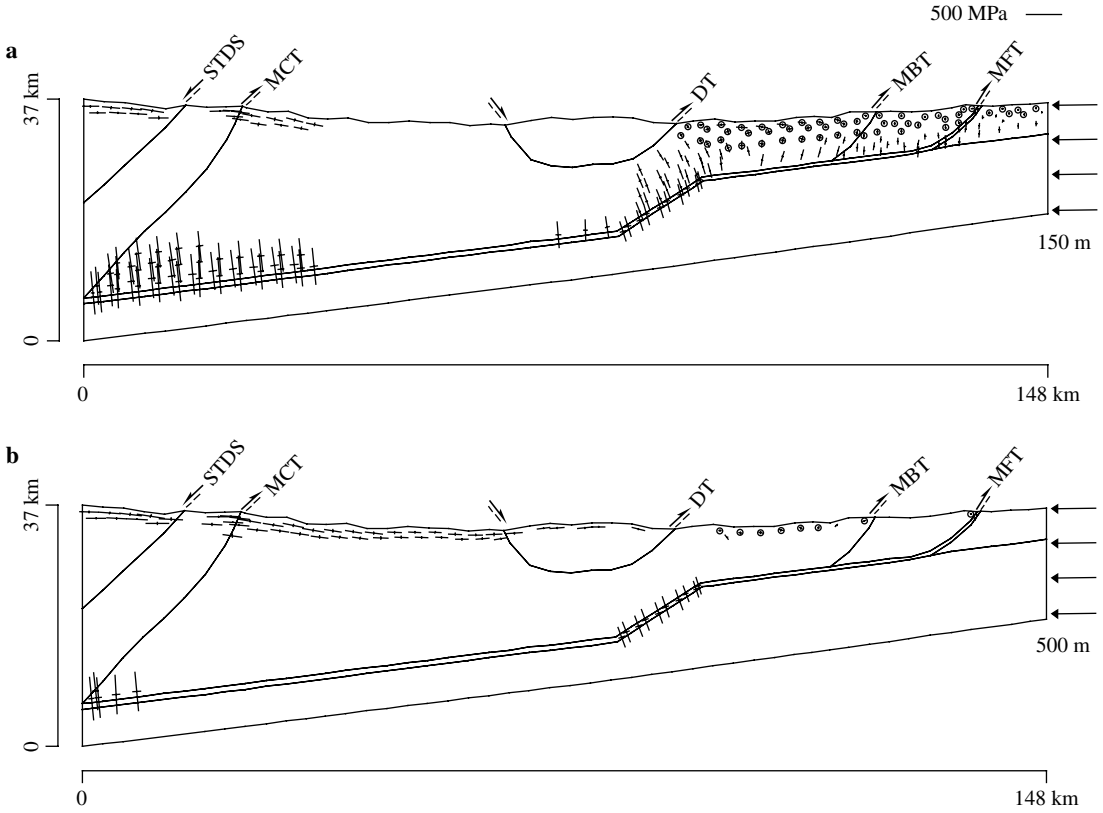


Fig. 15. Failure elements in the western Nepal model: (a) at 150 m convergent displacement; (b) at 500 m convergent displacement. Every pair of perpendicular lines represents σ_1 (long lines) σ_3 (short lines) in failure elements. The tensional stress field is shown by open circles. Abbreviations are same as Fig. 6.

active faults and seismicity in the fold-and-thrust belt of the Nepal Himalaya. Comparing the results of modeling with the available data of the active faults and microseismicity, we draw following conclusions:

1. Neotectonic stress field in the Himalaya is governed mainly by the geometry of the MHT. The area to the north of the mid-crustal ramp is in compressive stress state, whereas the area to the south is in a tensional stress field. This difference in the stress field is attributed to the presence of the mid-crustal ramp along the MHT.
2. Shear stress accumulation along the northern flat of the MHT is induced entirely by the mid-crustal ramp, which acts as a geometrical asperity during interseismic periods. Since microseismic events are simply the local stress adjustments, accumulation of the shear stress along the northern flat indicates that the MHT will be reactivated in the next large ($M_w > 8$) earthquake.
3. The simulated fault pattern corresponds to several active normal faults in Nepal Himalaya. Normal faults results from the change in stress field due to the formation of a mid-crustal ramp along the MHT.
4. The direction of thrust propagation is in good agreement with the sequence of thrusting in the Himalaya.
5. Failure elements along the flat–ramp–flat coincide with the microseismicity of the central and western Nepal. These microseismic events are considered to release a part of the elastic stress accumulated around the mid-crustal ramp during interseismic periods.

Acknowledgements

DC is indebted to the Ministry of Education, Culture, Sports, Science and Technology (Monbukagakusho) Japan, for financial support to carry out this research. We are grateful to Dr François Jouanne, who permitted us to use his figure. We thankfully acknowledge constructive comments and corrections from Dr A.J. Barber, University of London and two anonymous reviewers. We are equally thankful to guest editors (Profs. K. Arita, A. Yin, H. Okada and Dr S. Singh) and the editorial board for their efforts to bring this issue.

References

Barton, P.J., 1986. The relationship between seismic velocity and density in continental crust — a useful constraint? Geophysical Journal Royal Astronomical Society 87, 195–208.

Beaumont, C., Fullsack, P., Hamilton, J., 1994. Styles of crustal deformation in compressional orogens caused by subduction of the underlying lithosphere. Tectonophysics 232, 119–132.

Berger, A., Jouanne, F., Hassani, R.D., Mugnier, J.L., 2004. Modelling the spatial distribution of the present-day deformation in Nepal: how cylindrical is the main Himalayan thrust in Nepal? Geophysical Journal International 156, 94–114.

Bott, M.H.P., Waghorn, G.D., Whittaker, 1989. Plate boundary forces at subduction zones and trench-arc compression. Tectonophysics 170, 1–15.

Brunel, M., 1986. Ductile thrusting in the Himalayas: shear sense criteria and stretching lineations. Tectonics 5, 247–265.

Cattin, R., Avouac, J.P., 2000. Modelling mountain building and the seismic cycle in the Himalaya of Nepal. Journal of Geophysical Research 105, 13389–13407.

Chamlagain, D., Hayashi, D., 2004. Numerical simulation of fault development along NE–SW Himalayan profile in Nepal. Journal of Nepal Geological Society 29, 1–11.

Chamlagain, D., Kumahara, Y., Nakata, T., Upreti, B.N., 2000. Active faults of Nepal Himalaya with references to Himalayan frontal fault and their neotectonic significance. Proceedings of QUCTEHR. Kumaon University, India, pp. 124–125.

Chapple, W.M., 1978. Mechanics of thin-skinned fold-and-thrust belts. Geological Society of America Bulletin 89, 1189–1198.

Cotton, F., Campillo, M., Deschamps, A., Rastogi, B., 1996. Rupture history and seismotectonics of the 1991 Uttarkashi Himalaya earthquake. Tectonophysics 258, 35–51.

Dahlen, F.A., 1990. Critical taper model of fold-and-thrust belts and accretionary wedges. Annual Review of Earth and Planetary Sciences 18, 55–99.

Davis, D., Suppe, J., Dahlen, F.A., 1983. Mechanics of fold-and-thrust belts and accretionary wedges. Journal of Geophysical Research 88, 1153–1172.

Decelles, P.G., Robinson, D.M., Quade, J., Ojha, T.P., Garzione, C.N., Copeland, P., Upreti, B.N., 2001. Stratigraphy, structure, and tectonic evolution of the Himalayan fold-thrust belt in western Nepal. Tectonics 20, 487–509.

Erickson, S.G., Stryer, L.M., Suppe, J., 2001. Initiation and reactivation of faults during movement over a thrust-fault ramp: numerical models. Journal of Structural Geology 23, 11–23.

Hayashi, D., Fujii, Y., Yoneshiro, T., Kizaki, K., 1984. Observations on the geology of the Karnali region, west Nepal. Journal of the Nepal Geological Society 4, 29–40.

Jouanne, F., Mugnier, J.L., Gamond, J.F., Le Fort, P., Pandey, M.R., Bollinger, L., Flouzat, M., Avouac, J.P., 2004. Current shortening across the Himalayas of Nepal. Geophysical Journal International 157, 1–14.

Kumahara, Y., Upreti, B.N., Chamlagain, D., Nakata, T., 2001. Active faults along the Himalayan front in eastern and central Nepal. ILP, New Zealand.

Lallemand, S.E., Schnürle, P., Malavieille, J., 1994. Coulomb theory applied to accretionary and nonaccretionary wedges: possible causes for tectonic erosion and/or frontal accretion. Journal of Geophysical Research 99, 12033–12055.

Lave, J., Avouac, J.P., 2000. Active folding of fluvial terraces across the Siwaliks Hills, Himalayas of central Nepal. Journal of Geophysical Research 105, 5735–5770.

Mäkel, G., Walters, J., 1993. Finite-element analyses of thrust tectonics: computer simulation of detachment phase and development of thrust faults. Tectonophysics 226, 167–185.

Mandl, G., Shippam, G.K., 1981. Mechanical model for thrust sheet gliding and imbrication. In: McClay, K.R., Price, N.J. (Eds.), Thrust and Nappe Tectonics. Geological Society, Special Publication, London, pp. 79–98.

Mikhailov, V.O., Smolyaninova, E.I., Sebrier, M., 2002. Numerical modeling of the neotectonic movements and the state of stress in the North Caucasus foredeep. Tectonics 21. doi:10.1029/2002TC001379.

Mugnier, J.-L., Huyghe, P., Chalaron, E., Mascle, G., 1994. Recent movements along the main boundary thrust of the Himalayas: normal faulting in an over-critical wedge? Tectonophysics 238, 199–215.

Nakata, T., 1982. A photogrammetric study on active faults in the Nepal Himalayas. Journal of the Nepal Geological Society 2, 67–80.

Nakata, T., 1989. Active faults of the Himalaya of India and Nepal. Geological Society of America Special Paper 232, 243–263.

Nakata, T., Kumahara, Y., 2002. Active faulting across the Himalaya and its significance in the collision tectonics. Active Fault Research 22, 7–16.

Nakata, T., Iwata, S., Yamanaka, H., Yagi, H., Maemoku, H., 1984. Tectonic landforms of several active faults in the western Nepal Himalayas. Journal of the Nepal Geological Society 4, 177–200.

Nakata, T., Otsuki, K., Khan, S.H., 1990. Active faults, stress field, and plate motion along the Indo-Eurasian plate boundary. Tectonophysics 181, 83–95.

Ni, J., Barazangi, M., 1984. Seismotectonics of the Himalayan collision zone: geometry of the underthrusting Indian plate beneath the Himalaya. Journal of Geophysical Research 89, 1147–1163.

Pandey, M.R., Tandukar, R.P., Avouac, J.P., Lave, J., Massot, P., 1995. Interseismic strain accumulation on the Himalayan crustal ramp (Nepal). Geophysical Research Letters 22, 751–754.

Pandey, M.R., Tandukar, R.P., Avouac, J.P., Vergne, J., Heritier, Th., 1999. Seismotectonics of the Nepal Himalaya from a local seismic network. Journal of Asian Earth Sciences 17, 703–712.

Patrait, P., Achache, J., 1984. India–Eurasia collision chronology and its implications for crustal shortening and driving mechanisms of plates. Nature 311, 615–621.

Pauselli, C., Federico, C., 2003. Elastic modeling of the Alto Tiberina normal fault (central Italy): geometry and lithological stratification influences on the local stress field. Tectonophysics 374, 99–113.

Saijo, K., Kimura, K., Komatsubara, T., Yagi, H., 1995. Active faults in southwestern Kathmandu basin, central Nepal. Journal of the Nepal Geological Society 11, 217–224.

Sassi, W., Faure, J.-L., 1997. Role of faults and layer interfaces on the spatial variation of stress regimes in basins: inferences from numerical modelling. Tectonophysics 266, 101–119.

Schelling, D., Arita, K., 1991. Thrust tectonics, crustal shortening and the structure of the far eastern Nepal Himalaya. Tectonics 10, 851–862.

Singh, R.P., Li, Q., Nyland, E., 1990. Lithospheric deformation beneath the Himalayan region. Physics of the Earth and Planetary Interiors 61, 291–296.

Srivastava, P., Mitra, G., 1994. Thrust geometries and deep structure of the outer and Lesser Himalaya, Kumaon and Garhwal (India): Implications for evolution of the fold-and-thrust belt. Tectonics 13, 89–109.

Sydney, P., Clark, J.R. (Eds.), 1966. Handbook of Physical Constants. Geological Society of America Memoir, Vol. 97, 587 p.

Upreti, B.N., Le Fort, P., 1999. Lesser Himalayan crystalline nappes of Nepal: problem of their origin. In: Macfarlane, A., Quade, J., Sorkhabi, R. (Eds.), Geological Society of America Special Paper, 328, pp. 225–238.

Vanbrabant, Y., Jongmans, D., Hassani, R., Bellino, D., 1999. An application of two-dimensional finite-element modelling for studying the deformation of the Variscan fold-and-thrust belt (Belgium). Tectonophysics 309, 141–159.

Vergne, J., Cattin, R., Avouac, J.P., 2001. On the use of dislocations to model interseismic strain and stress build-up at the intracontinental thrust faults. Geophysical Journal International 47, 155–162.

Wang, C., Shi, Y., 1982. On the tectonics of the Himalaya and Tibet plateau. Journal of Geophysical Research 87, 2949–2957.

Willet, S., Beaumont, C., Fullsack, P., 1993. A mechanical model for the tectonics of doubly vergent compressional orogens. Geology 21, 371–374.

Wiltschko, D.V., 1979. A mechanical model for thrust sheet deformation at a ramp. Journal of Geophysical Research 84, 1091–1104.

Zhao, W., Nelson, K.D., Project INDEPTH Team, 1993. Deep seismic reflection evidence for continental underthrusting beneath southern Tibet. Nature 366, 557–559.